14th Australasian Fluid Mechanics Conference
Adelaide University, Adelaide, Australia
10-14 December 2001

Effect of Initial Conditions on the Turbulence Structures Various Scales in a Self-Preserving Wake

Yu ZHOU[1] and Hui LI[2]
[1]Department of Mechanical Engineering
The Hong Kong Polytechnic University, Hung Hom, Kowloon, Hong Kong
[2]Department of Mechanical Engineering
Kagoshima University, 1-21-40, Korimoto, Kagoshima 890-0065, JAPAN

Abstract

Initial condition effects in a self-preserving plane wake have been investigated for two wake generators, i.e. a circular cylinder and a screen of 50% solidity. The experimental investigation uses two orthogonal arrays of sixteen X-wires, eight in the (x, y)-plane, i.e. the plane of mean shear, and eight in the (x, z)-plane, which is parallel to both the cylinder axis and the streamwise direction. The two arrays allow velocity data to be obtained simultaneously in the two planes. Measurements were made at x/h (x is the streamwise distance downstream of the cylinder and h is the height of the wake generator) = 280 for the circular cylinder and 220 for the screen. The wake has been previously verified to be approximately self-preserving at these downstream stations. The effect of initial conditions on turbulence structures has attracted considerable attention in the literature. Previous studies suggested that the characteristics of the organised motion in a self-preserving wake could differ as initial conditions vary. Most of these investigations focus on large-scale structures; the role of turbulence structures of other scales has yet to be clarified since it is difficult to extract the structures of these scales using conventional vortex-detection techniques. In the present investigation, a two-dimensional orthogonal wavelet transform is used to analyse the measured hot-wire data. This technique enables the turbulence structures of various scales to be separated and characterised. Discernible differences are observed between the two wake generators in the turbulence structures of large- down to intermediate-scales. The differences are quantified in terms of the Reynolds shear stress, kinetic energy and root mean square vorticity values.

Introduction

There has been accumulating experimental evidence that points to the persistence of initial conditions in the self-preserving region of a turbulent flow. Most of the evidence has been obtained in plane and axi-symmetric wake flows. Bevilaqua and Lykoudis [1] compared the wake of a sphere with that of a porous disk which had the same drag and Reynolds number ($Re_h = U_\infty h/\nu$ = 10,000, where U_∞ is the free stream velocity, h is the characteristic height and ν is the kinematic viscosity). They observed that the turbulence intensity, normalised by the maximum velocity deficit U_1, was greater in the wake of the sphere than in that of the disk. They proposed a hierarchy of self-preserving states, i.e. order one when the mean velocity reaches self-preservation, order two when Reynolds stresses become self-preserving in addition to the mean velocity, and so on through higher order moments. George [6] also proposed a similar concept. Wygnanski [15] examined turbulent plane wakes (x/θ = 100 ~ 2000, where x is the streamwise co-ordinate and θ is the momentum thickness) behind various generators of approximately the same drag coefficient. They observed a dependence of the normalised longitudinal turbulence intensity $\overline{u^2}$ and Reynolds shear stress $\overline{uv}$ on initial conditions in the self-preserving region. The studies by Bonnet et al. [2], Louchez et al. [10] and Cimbala et al. [3] have confirmed that the detailed behaviour of a turbulent far-wake can depend on initial conditions.

It has been argued that there is a link between self-preservation and large-scale organised structures (George [6]; Bevilaqua and Lykoudis [1]). The persistence of the effect of initial conditions in the self-preserving region seems to imply that the characteristics of the large-scale organised structures depended on initial conditions. Using a vorticity-based detection scheme, Zhou and Antonia [14] educed large-scale vortical structures in a self-preserving wake produced by different generators (circular, triangular, square cylinder and a screen). Conditional sectional streamlines and contours of the shear stress indicated that the large-scale vortical structures in the self-preserving screen wake are more asymmetrical than in the self-preserving solid-body wakes. Accordingly, the contribution to the Reynolds shear stresses is appreciably larger in the screen wake than in the solid-body wakes. However, Zhou & Antonia's detection scheme could not identify organised structures other than the large-scale ones. It is suspected that the organised structures of various scales all contribute to the dependence of a self-preserving wake on the initial conditions.

The main objective of the present work is to study the effect of initial conditions on the turbulence structures of various scales. The experimental investigation uses two orthogonal arrays of sixteen X-wires, eight in the (x, y)-plane and eight in the (x, z)-plane. The two arrays allow velocity data to be obtained simultaneously in the two planes. Measurements were conducted in the far-wake generated by a circular cylinder and a screen of 50% solidity, respectively. A wavelet analysis technique (Li [8]) was used to decompose the data into a number of subsets based on their characteristic central frequencies or scales. The circular cylinder far-wake is compared with that generated by the screen in terms of contributions to Reynolds stresses from different subsets. The contribution is also examined to the root mean square (rms.) vorticity from the structures of different scales.

Experimental Details

Experiments were carried out in an open return low turbulence wind tunnel with a 2.4 m long working section (0.35 m x 0.35 m). The bottom wall was tilted to achieve a zero streamwise pressure gradient. A circular cylinder (h = 6.35 mm) and a screen (h = 8.0) of 50% solidity were used to generate the wake, respectively; each was installed in the mid-plane and spanned the full width of the working section, 0.20 m from the exit plane of the contraction. The two generators corresponded to a blockage of 1.8% and 1.2%, respectively. Measurements were made at U_∞ = 6.7 m/s, resulting in different Reynolds number for the two generators. Table 1 summarises flow parameters for the two wake generators, where L is the half width, and Re_θ is the Reynolds number based on θ.. The wake has been verified to reach approximately the state of self-preservation (Zhou & Antonia [14]). Ideally, the measurements should have been made for the same blockage ratio and Reynolds number. This would be difficult to achieve. Nevertheless, the far wake is unlikely to depend strongly on Re_h or Re_θ given a sufficiently large Reynolds number.

Wake generator	h (mm)	θ (mm)	Re_d	Re_θ	L (mm)	U_1/U_∞ (%)	x/d	x/θ
Cylinder	6.35	3.0	2,800	1,350	25	6.9	280	580
Screen	8.00	2.1	3600	900	15.5	6.3	220	830

Table 1. Characteristic wake parameters

Using two orthogonal arrays, each comprising eight X-wires (Figure 1), velocity fluctuations *u, v* in the (*x, y*)-plane and *u, w* in the (*x, z*)-plane were obtained simultaneously. The nominal spacing between X-wires in both planes was about 5 mm except for a relatively large gap (= 9.1 mm) between the fourth and fifth X-wires in the (x, z)-plane. The arrays were attached to separate traversing mechanisms and could be moved independently of each other. The eight X-wires in the (*x, y*)-plane were fixed with the second X-wire (from the bottom) positioned approximately on the centreline; the eight X-wires in the (*x, z*)-plane was located at about 10 mm above the centreline. The data obtained in the (*x, z*)-plane were not used presently. The physical blockage caused by these arrays, cables and supports was estimated to be about 3%. Several types of measurements (Zhou & Antonia, [12]) indicated that the interference to the flow due to the two arrays was negligible.

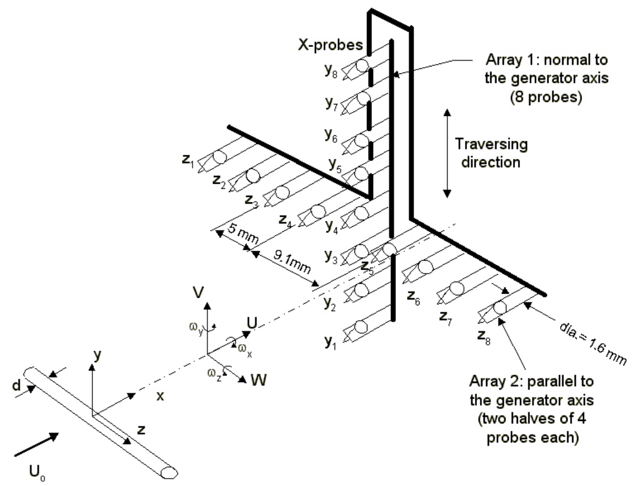

Figure 1 Experimental arrangement

Wollaston (Pt-10% Rh) wires, 5 µm in diameter and about 1 mm in working length, were operated with constant temperature circuits. Signals from the circuits were offset, amplified and then digitised using two 16 channel (12bit) A/D boards and two personal computers at a sampling frequency of 3.5 kHz per channel (the cut-off frequency was 1600Hz). Data acquisition by the two computers was synchronized using a common external trigger pulse. The wires were calibrated for velocity and yaw, and continuously checked for drift. Using velocity and yaw calibrations, signals proportional to *u*, *v* and *w*, together with the local mean velocities $\overline{U}$, $\overline{V}$ (≈ 0) and $\overline{W}$ (≈ 0), were recorded in a computer. The duration of each record was about 38 sec.

Decomposition of Turbulence Structure into Various Scales

The wavelet analysis enables a non-linear problem to be transformed to the superposition of linear problems (e.g. Mallat [11]), which started to receive the attention of researchers in fluid mechanics and turbulence about one decade ago (Farge [5]). There is recently an increasing interest in applying this mathematical tool to the analysis of the organised structures in turbulent flows. In the present application, a vector wavelet multi-resolution analysis technique is used to analyse the measured velocity data. This technique was discussed in detail, for example, in Li [8] and Li and Zhou [9] and therefore is not repeated here. Briefly, the Daubechies family (Daubechies [4]) with index N = 20 is chosen for orthogonal wavelet basis to construct the wavelet space. An instantaneous velocity F can be written as the sum of a time-averaging component $\overline{F}$ and a fluctuating component f, viz.

$$F = \overline{F} + f \tag{1}$$

The velocity fluctuation component f is decomposed into a number of subsets based on wavelet levels, which correspond to the central frequencies or scales. Thirteen wavelet levels are used presently and f may be given by

$$f = \sum_{i=1}^{13} f_i \,, \tag{2}$$

where f_i is the component of f in the *ith* subset. Accordingly, the instantaneous velocity in the *ith* subset is given by

$$F_i = \overline{F} + f_i \tag{3}$$

Vorticity approximation may be obtained based on velocity data using the central difference approximation (Hussain and Hayakawa, [7]). Thus, the eight X-wires in each plane may produce vorticity data at each of the seven midpoints between adjacent X-wires. The spanwise vorticity component in the *ith* subset may be approximated by

$$\omega_{zi} = \frac{\partial V_i}{\partial x} - \frac{\partial U_i}{\partial y} = \frac{\partial v_i}{\partial x} - \frac{\partial(\overline{U} + u_i)}{\partial y}$$
$$\approx \frac{\Delta v_i}{\Delta x} - \frac{\Delta(\overline{U} + u_i)}{\Delta y} \tag{4}$$

where $U_i = \overline{U} + u_i$ and $V_i \approx v_i$ ($\overline{V} \approx$ 0). In Eq. (4), Δy (≈*5.0mm*) is spacing between two X-wires in the (*x, y*)-plane; $\Delta x = -\overline{U}\,\Delta t = -\overline{U}/f_s$. For simplicity, $\overline{U} = 0.94U_\infty$ on the vortex path (Zhou & Antonia [13]) is used to calculate Δx. Vorticity contours and rms. values thus obtained showed no appreciable difference from those obtained using the local mean velocity.

Results and Discussion

Figure 2 presents the lateral distributions of time-averaged Reynolds stresses and the subsets, obtained from the vector wavelet multi-resolution analysis, at different wavelet levels or central frequencies. The results are normalized by the maximum value of the measured time-averaged stresses $(\overline{fg})_{\max}$, where f or g may each represent u or v, so as to indicate the contribution from each subset or central frequency to the Reynolds stresses. The negative $(\overline{uv})_i/(\overline{uv})_{\max}$ near y/L = 0 and at relatively high central frequencies has been removed in Figure 2c to allow the log-scale presentation. The $(\overline{fg})_{\max}$ values (Table 2) show discernible difference between the circular-cylinder and the screen wakes, in particular for $(\overline{u^2})_{\max}$. The observation is in consistence with Zhou & Antonia (1995)'s report, suggesting the effect of different generators. The power spectrum (not shown) of the v-signal exhibits a prominent peak around the frequency f_0, which is 65Hz and 120Hz in the circular cylinder and screen wakes, respectively. The subset of the central frequency f_0 may therefore represent the large-scale vortical structures. The sectional streamlines and vorticity contours (not shown here) of the subset display a flow pattern similar to the conditional averaged results (Zhou & Antonia [13]; [14]), thus providing a validation of the present used data analysis technique.

The total contribution from the subsets of f_0, $2f_0$, $4f_0$ and $8f_0$ accounts for about 70% of $\overline{u^2}$, 90% of $\overline{v^2}$ and 85% of $\overline{uv}$. The error caused by neglecting the frequencies higher than $8f_0$ is negligible. The deficit is mostly due to the chop off of the frequencies lower than f_0. The power spectrum of the *u* signal exhibits significant energies at frequencies lower than f_0, which explains the relatively large deficit between $\overline{u^2}$ and the contribution from the subsets.

The maximum value of $(\overline{fg})_i/(\overline{fg})_{\max}$ corresponding to f_0 is between 50% and 60% of the measured $\overline{fg}$, slightly higher than the maximum coherent contribution from the large-scale vortical structures, as given in Table 2 of Zhou & Antonia [14]). The value of $(\overline{fg})_i/(\overline{fg})_{\max}$ decreases as the central frequency increases, consistent with the perception that the lower frequency eddies are energy-containing. The decrease is rather rapid, up to 25 ~ 35% of the measured $\overline{fg}$, when the central frequency increases from f_0 to $2f_0$. Nevertheless, the Reynolds stresses associated with $2f_0$ is still significant, ranging between 15% and 25% of the measured $\overline{fg}$. This indicates a significant contribution, from the intermediate-scale structures to the total Reynolds stresses. For the central frequency greater than $4f_0$, $(\overline{fg})_i/(\overline{fg})_{\max}$ tends to fall off quickly, approaching zero.

	$\overline{u^2}$	$\overline{v^2}$	$\overline{uv}$	$\omega_{z,rms}$
Circular cylinder	0.023	0.014	- 0.008	1.53x10^{-3}
Screen	0.018	0.013	-0.006	1.63x10^{-3}

Table 2 Maximum values of $\overline{u^2}$, $\overline{v^2}$, $\overline{uv}$ and $\omega_{z,rms}$

The $(\overline{fg})_i/(\overline{fg})_{\max}$ value of f_0 in the screen wake is larger than that in the circular cylinder wake (not so evident in Figure 2 because of the use of log scale). The observation conforms to Zhou & Antonia [14] report that the coherent contribution from the large-scale vortical structures to the Reynolds stresses is larger in the screen far-wake than in the solid body far-wake. The result again confirms the conception that the large-scale vortical structures contribute to the effect of initial conditions on the self-preserving wake. Furthermore, the difference between the two wakes is appreciable down to the subsets of $4f_0$, suggesting that the intermediate-scale structures also play a role in the persistence of the initial conditions.

Figure 3 presents the spanwise rms. vorticity, $\omega_{z,rms}/(\omega_{z,rms})_{\max}$, and the wavelet subsets, $(\omega_{z,rms})_i/(\omega_{z,rms})_{\max}$, calculated from Eq (4). Interpolation was used to add data between those obtained from Eq (4). The total contribution from the included subsets accounts for barely 70% of the rms. value. The deficit is largely due to the chop off of the frequencies lower than f_0 and higher than $8f_0$. For the circular cylinder, $(\omega_{z,rms})_i/(\omega_{z,rms})_{\max}$ corresponding to f_0 is now smallest, about 20% of the total rms. vorticity, among the subsets, while that at $4f_0$ is largest. This trend is reversed for the screen wake. In view of a relatively large uncertainty, about 20%, in the estimate of vorticity, the trend exhibiting here may not be trustworthy. Nevertheless, the observation could suggest that the intermediate- and relatively small-scale structures make an important contribution to the total rms. vorticity. With the caveat of a large uncertainty associated with vorticity estimate, the difference in $(\omega_{z,rms})_i/(\omega_{z,rms})_{\max}$ between the screen and circular cylinder wakes is again appreciable.

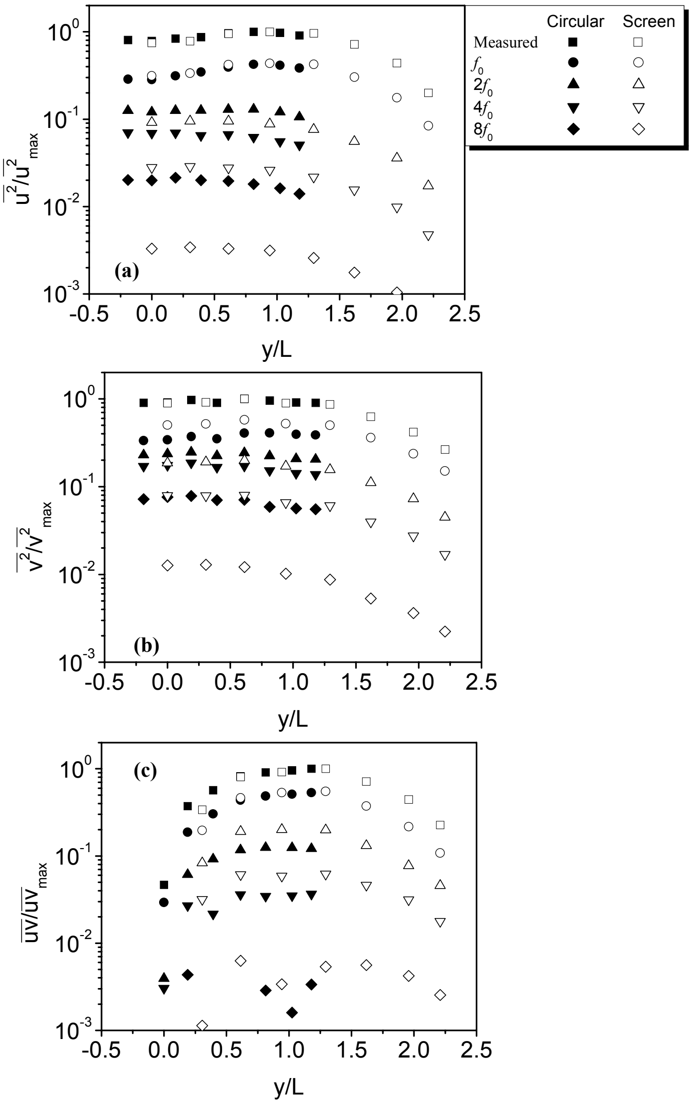

Figure 2 Reynolds stresses of the measured and the wavelet subsets at various central frequencies

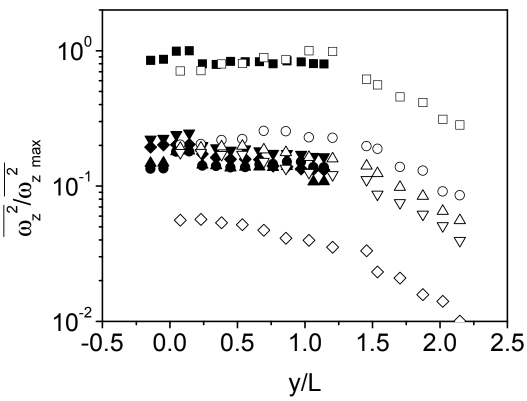

Figure 3 Spanwise rms vorticity of the wavelet subsets at various central frequencies. The symbols are as in Figure 2.

Conclusion

The self-preserving wake generated by a screen and a circular cylinder, respectively, has been investigated with a view to provide information on the possible effect of initial conditions on turbulence structures of various scales. Zhou & Antonia [14] have previously observed that Reynolds stresses, spectra and rms. vorticity distributions in the two wakes were not universal. The report, together with various experimental observations (e.g. Wygnanski et al. [15]) and the theoretical analysis (George [6]), pointed to a persistence of initial conditions. Zhou & Antonia also confirmed that the large-scale vortical structures in the self-preserving wake depended on the wake generator. In the present investigation, an orthogonal wavelet multi-resolution technique is applied to analyse the velocity data obtained in the two wakes. The data is decomposed into thirteen subsets based wavelet levels, or central frequencies/scales. The subset of the central frequency corresponding to the large-scale structures exhibits behaviours similar to the large-scale structures in terms of contributions to the Reynolds stresses and shows a difference between the two wakes. This reconfirms the dependence of the large-scale structures on the wake generator. Furthermore, the subsets up to four times the central frequency of large-scale structures also display discernible difference between the two wakes, indicating an effect of initial conditions on intermediate-scale structures as well as large-scale ones.

Acknowledgments

Y. Zhou wishes to acknowledge support given to him by the Research Grants Council of the Government of the HKSAR through Grant PolyU5125/98E.

References

[1] Bevilaqua, P.M. and Lykoudis, P.S., Turbulence memory in self-preserving wakes, *Journal of Fluid Mechanics,* **80**, 1978, 589-606.

[2] Bonnet, J-P., Delville, J. and Garem, H., Space and space-time longitudinal velocity correlations in the turbulent far wake of a flat plate in incompressible flow, *Experiments in Fluids,* **4**, 1986, 189-196.

[3] Cimbala J. M., Nagib H.M., Roshko A., Large structure in the far wakes of two-dimensional bluff bodies. *Journal of Fluid Mechanics,* 19**0**, 1988, 265-298.

[4] Daubechies I., Ten Lectures on Wavelets. *Society for Industrial and Applied Mathematics, 1992*.

[5] Farge M., Wavelet Transforms and Their Applications to Turbulence. *Annu. Rev. Fluid Mech.* **24**, 1992, 395-457.

[6] George, W.K., The self-preservation of turbulent flows and its relation to initial conditions and coherent structures, in W.K.George and R.Arndt (eds.). *Advances in Turbulence,* Berlin, Springer, 1989, 39-74.

[7] Hussain A.K.M.F. & Hayakawa M., Education of large-scale organized structures in a turbulent plane wake. *Journal of Fluid Mechanics,* **180**, 1987, 193-229.

[8] Li H., Identification of Coherent Structure in Turbulent Shear Flow with Wavelet Correlation Analysis. *ASME Journal of Fluids Engineering,* **120**, 1998, 778-785.

[9] Li, H. and Zhou, Y., Multi-Scale Structures in a Turbulent Near-Wake. *Advances in Turbulence VIII*, CIMNE publishers, Spain, 2000, 245-248.

[10] Louchez, P.R., Kawall, J.G. and Keffer, J.F., Detailed spread on characteristics of plane turbulent wakes, *Proc. 5th Symposium on turbulent shear flows*, Lecture Notes in Physics, Springer, 1987, 98-109.

[11] Mallat S., A Theory for Multi-resolution Signal Decomposition: The Wavelet Representation. *IEEE Trans.* PAMI **11**, 1989, 674-693.

[12] Zhou Y. & Antonia R.A., Critical points in a turbulent near-wake. *Journal of Fluid Mechanics,* **275**, 1994a, 59-81.

[13] Zhou, Y. & Antonia, R. A., " Effect of Initial Conditions on Structures in a Turbulent Far-Wake", *Journal of JSME,* **37**, 1994b, 718-724 (invited paper).

[14] Zhou, Y. & Antonia, R. A., "Memory Effects in Turbulent Plane Wakes", *Experiments in Fluids*, **19,** 1995, 112-120.

[15] Wygnanski, I., Champagne, F. and Marasli, B., On the large-scale structures in two-dimensional, small-deficit, turbulent wakes, *Journal of Fluid Mechanics*, **168**, 1986, 31-71.